



Effect of treatment time and temperature on microstructure and corrosion behavior of Zn-Ni electrophosphosphate coating

Ghasem Barati Darband ^{a,*}, Abdollah Afshar ^a, Majid Rabani ^b

^a Department of Material Science and Engineering, Sharif University of Technology, Tehran, Iran

^b Esfarayen University of Technology, Esfarayen, Iran

ARTICLE INFO

Article history:

Received 1 April 2016

Received in revised form

23 June 2016

Accepted 3 July 2016

Available online 5 July 2016

Keywords:

Electrophosphating

Zn-Ni

SEM

Polarization

EIS

ABSTRACT

In this study, the effect of phosphating time and temperature on microstructure and corrosion behavior of Zn-Ni electrophosphosphate coating with a galvanized steel as a substrate, were investigated. SEM and X-ray diffraction methods were used for investigation the microstructure and phase analysis, respectively. And immersion test, potentiodynamic polarization test, and Electrochemical Impedance Spectroscopy tests were used for the study of corrosion behavior. The results of this study indicated that the best coating morphology is obtained in the range between 20 and 30 min and 40–50 °C. Moreover, results of corrosion studies showed that the corrosion mechanism is under diffusion control due to the formation of zinc base corrosion products.

© 2016 Elsevier B.V. All rights reserved.

1. Introduction

Due to the poor corrosion resistance of iron in the atmosphere, zinc coatings are commonly applied on steel surface in order to enhance the corrosion resistance of plain steels through a barrier and sacrificial protection [1,2]. However, the corrosion product of zinc coating formed in the atmosphere cannot provide sufficient protection for steel substrates. For better protection of zinc-coated steel against corrosion, surface reformation is generally applied to galvanized steel. Phosphating is one of the most indispensable processes which is used for solving this problem [3–6]. Phosphating is the most applicable metal pretreatment process for surface treatment and finishing of ferrous and non-ferrous metals. The main purpose of this process is corrosion protection, assisting cold forming of the metals, improving abrasion resistance, insulation, decoration applications and also used as pretreatment for increase paint adhesion to underlying metal [7–10].

Most phosphating baths which reported in the literature, require high operation temperature ranging from 80 to 90 °C. The main disadvantage of these baths is high energy consumption which is the main crisis in the world. Furthermore, using and

maintaining of heating coils of high-temperature bath is difficult due to the scale formation which leads to undesirable heating of the bath and consequently frequent replacement is required. Another critical problem occurs during high-temperature phosphating treatment is overheating of the bath which gives rise to the fast conversion of primary phosphate to tertiary phosphate before the metal is treated. These reasons lead to increase in free acidity of the bath and then delay the precipitation of the phosphate coating. One of the solutions to these problems is using of low-temperature phosphating bath. Nonetheless the low-temperature phosphating treatments are very slow and must be accelerated by some procedures. Chemical, electrochemical and mechanical procedures are used for accelerating the phosphating treatments. In most cases, the chemical accelerator is used in many industries, but a vast number of the chemical accelerators are classified as toxic materials, so using the chemical accelerator can be detrimental to the environment [11–15]. Electrochemical methods for accelerating of phosphating treatment is developed for achieving the coating with a high thickness in low temperature and time treatment. As in this treatment, electrical current served as an accelerator, by applying current, chemical accelerator can be removed from the bath.

The presence of an additives such as Ni ions in the bath bring about improvement in corrosion resistance of the coating due to the decrease in grains of the coating. Another reason for improving the corrosion resistance in the presence of Ni is the formation of Ni-

* Corresponding author.

E-mail address: q.barati70@yahoo.com (G.B. Darband).

rich alloy in the bottom of the pores [16–18]. There are many factors affecting properties of phosphate coatings such as the pH of the bath, the additives concentration in the bath, time and temperature of the bath. Effect of coating parameters and conditions on phosphate coating are investigated by many researchers [19–21]. Li, G. Y., et al. [22] have indicated that the microstructure of the conventional phosphate coating is very dependant on pH and the best microstructure was obtained at very close pH range. However, the effect of coating parameters and conditions of electrophosphate coating on galvanized steel and achieving the best condition for favorable corrosion resistance and microstructure was never been studied. Therefore, in this study, the effect of treatment time and temperature on microstructure and corrosion behavior of Zn-Ni electrophosphate coating will be precisely investigated.

2. Experimental details

Hot-dip galvanized steel samples with a dimension of 50 mm × 20 mm × 2 mm were used as a substrate in this study, the thickness of zinc coating on steel substrate in galvanized steel was about 10 µm. The substrate was ultrasonically degreased in acetone for 12 min, then rinsed with de-ionized water and pickled in 4% H₂SO₄ for 20 s. Activation of samples was performed by dipping into a titanium phosphate solution (1 g/lit) for 1 min [5]. Prepared specimens finally immersed into a phosphating solution contained in the cell at different coating conditions. A galvanostat was used to apply constant direct current to Electrophosphating cell. The chemical composition and operating conditions of the bath are shown in Table 1. Stainless steel anodes were used in this study. Two sets of them were placed on both sides of the hot-dip galvanized steel substrate. Schematic of the cell used for electrophosphating treatment is shown in Fig. 1. The deposition of phosphate coating is carried out under galvanostatic condition. After the coating process, the coated samples were removed from the bath and then rinsed with de-ionized water to eliminate residual acids and salt on the surface of coated substrate and then dried using an air stream. The corrosion resistance of phosphate substrates was evaluated using immersion test potentiodynamic polarization and electrochemical impedance spectroscopy tests. Electrochemical measurements were performed by a model 273 A potentiostat/galvanostat and using 3.5% sodium chloride solution maintained at 27 °C as the electrolyte medium. The tested zone area was 1 cm² and remaining areas were sealed. The corrosion evaluation cell consists of three electrodes in which coated hot-dip galvanized steel as the working electrode, stainless steel plate as the counter electrode and finally saturated calomel electrode (SCE) as reference one. The polarization potentiodynamic tests were carried out in the range of –300 mV (relative to OCP potential) to +300 mV at the scan rate of 1 mV/Sec. The corrosion potential (E_{corr}), corrosion current density (i_{corr}) and anodic/cathodic Tafel constant (β_a and β_c) were evaluated using linear polarization

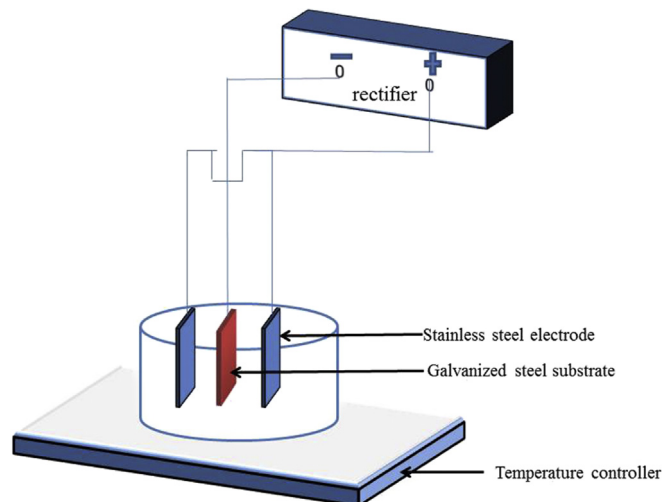


Fig. 1. Schematic of cell used for electrophosphating treatment.

method. The polarization resistance (R_p) can be determined from Stern-Geary equation based on the approximately linear polarization behavior near open-circuit potential (OCP) according to the following equation.

$$R_p = \frac{\beta_a \times \beta_c}{2.033(\beta_a + \beta_c)i_{corr}} \quad (1)$$

Impedance spectra were obtained at open circuit potential and the signal amplitude of measurement was 10 mV. The measuring frequency was 10^{–2}–10⁴ Hz. For each coating treatment three parallel experiments were done and average of them was selected for corrosion evaluation. Surface morphology and composition of the coating was characterized via scanning electron microscopy (SEM, model Vega, Tescan). To conduct the surface of samples, before SEM characterization, they were coated with Au. The crystal structure and phase of the coating were identified using X-ray diffraction method with Cu K α radiation. The thickness of coatings was measured using a nondestructive Fisher device (Dual Scope MP40 model) thickness measurement and each sample was carried out at 5 points and then average of those points were reported as thickness.

3. Results and discussion

3.1. Phase analysis and deposition mechanism

XRD pattern of Zn-Ni phosphate coating which formed using cathodic electrochemical method is presented in Fig. 2. As can be seen, Zn and Ni are present in the elemental form in the coating which formed using cathodic electrochemical method due to the applied cathodic current in this treatment. Zn and Ni are formed as a result of the reduction of Zn²⁺ and Ni²⁺ ions in the electrolyte based on following equations.



The Zn phase which appears in the XRD pattern also can be originated from the substrate. As can be seen, NiZn₃ phase also appears in the XRD pattern which can be formed according to the following equation under the effect of applied cathodic polarization on the metal surface during the coating process.

Table 1
Chemical composition and operating conditions of the bath.

Bath composition	Amount
ZnO(g/l)	2.04
H ₃ PO ₄ (ml/l)	11
NaF(g/l)	0.3
Ni(NO ₃) ₂ (g/l)	1
Operating conditions	
pH	1.8
Temperature(°C)	27–40–50–60
Time(min)	10–20–30–40
Current density(mA/cm ²)	20

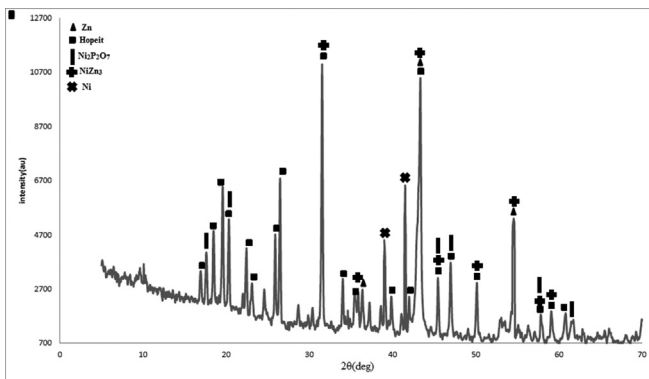


Fig. 2. XRD pattern of Zn-Ni phosphate coating obtained by cathodic electrochemical method.



In addition, Zn in the elemental form in the coating composition is reported by Jegannathan et al. [12], Narayanan et al. [14] and Oskuie et al. [23] in the Zn phosphating treatment using the cathodic electrochemical method. During the cathodic electrochemical phosphating treatment, by applying cathodic current on the metal surface, hydrogen evolution occurs according to the following reaction



Hydrogen evolution at the metal-electrolyte interface gives rise to increase in the interfacial pH. Rise in the interfacial pH triggers the conversion of soluble primary phosphate to insoluble tertiary phosphate based of following equation [24].



In which, $\text{Zn}_3(\text{PO}_4)_2$ is known as Hopeite which appears in the XRD pattern. It is believed that in the first step of Zn-Ni electro-phosphating, deposition of thin layer of Zn and Ni occur in conjunction with hydrogen evolution [25]. Then by rising interfacial pH at the metal-electrolyte interface, the formation of zinc and nickel phosphate phase occurs. Then, deposition of elemental zinc and nickel happen in the form of a channel which surrounding the phosphate phase. Therefore, Zn-Ni phosphate coating which formed using cathodic electrochemical method can be classified as Zn-Ni phosphate composite coating in which none metallic and metallic phase exist in the coating composition. These phases can strongly affect the corrosion behavior of resultant coating that will be discussed in the following sections.

3.2. Microstructure and kinetic of coating formation

3.2.1. Effect of phosphating temperature

The bath temperature is a critical factor which affects the microstructure of coating. The SEM micrograph of the coating formed at various bath temperatures is presented in Fig. 3. As can be seen, needle-like, flower-like and plate-like phosphate crystals appear at the coating surface. In order to identify the flower-like and plate-like crystals, EDS analysis was performed in the flower-like and plate-like regions and results of this analysis are presented in Fig. 4. As can be seen, the concentration of Ni in the plate-

like crystals (15.84%) is more than its concentration in flower-like crystals (1.18%). It can be inferred that the flower-like crystals are Hopeite and plate-like crystals are nickel phosphate. Generally it is believed that irrespective the method of phosphate coating deposition (chemical, electrochemical or sparing) the morphology of zinc phosphate-based coating appear to be either needle- or flower-like crystals [26]. The formation of needle-like phosphate crystals also have been reported by Flis et al. [27] in Zn-Ni chemical phosphate coating. Also, Banczek et al. [8] identified needle-like phosphate crystals in the zinc-nickel phosphating. It is evident from Fig. 3, morphological features of phosphate coating are varied with an increase in electrolyte temperature, as can be observed in Fig. 3a, at room temperature only small needle-like crystals formed on a substrate which doesn't cover the entire surface. Generally, the phosphate coating formation consists of nucleation and growth stages. In low temperature, the nucleation stage occur and small needle-like crystals are formed but at this temperature, the growth kinetics is too low, thus the growth step cannot complete. Fouladi et al. [20] also have indicated that in low temperature only a few crystals emerge after 20 min treatment in magnesium phosphate coating treatment. As can be seen, by rising the temperature to 40 °C, the kinetics energy of growth stage is high enough to complete the growth stage. In this temperature, the phosphate crystals completely cover the entire surface of the substrate. By increasing the temperature to 50 °C, remarkable changes do not occur and the surface is fully covered by phosphate crystals. By increasing the electrolyte temperature to 60 °C, an excessive rise in growth rate lead to the growth of pore between crystals and this fact causes the fabrication of coating with high porosity. The formed porosities are represented by an arrow in Fig. 3 d. high temperature assisted by applied cathodic current lead to improper coating formation at this situation, thus the best range for formation of a coating with the best microstructure is between 40 and 50 °C in the electro phosphating treatment.

3.2.2. Effect of phosphating time

Another factor that affects the microstructure of coating is the phosphating time treatment. SEM images of coating which fabricated at different treatment times are presented in Fig. 5 indicating the microstructure of coating which is affected by treatment time. As can be observed, flower-like and plate-like crystals are formed on the surface which was discussed in the previous section. In an initial time of phosphating (Fig. 5a), only small crystals islands are formed on a substrate which are not able to thoroughly cover the entire surface. The reason can be understood from the formation mechanism of the coating. As mentioned, in the initial stage of coating formation, a thin layer of Zn and Ni is formed and then by hydrogen evolution and rise in interfacial pH, primary phosphate convert to tertiary phosphate and phosphate crystals form on the thin layer of zinc and nickel which previously formed on the substrate. In the initial period of electrophosphating treatment, any color change cannot be observed at the substrate, and after 5 min the color of the substrate surface change to black, indicating the start of conversion of primary phosphate to tertiary phosphate and formation of phosphate crystals on the surface of the substrate. It can be concluded that before the color change of substrate, the deposition of thin Zn and Ni layer are the predominant reactions. Thus, in the sample, which coated in 10 min, most time of phosphating treatment have been devoted to the first stage in which the significant phosphate crystals are not formed. By increasing the phosphating time to 20 min, the surface is almost fully covered by phosphate crystals and the uniform coating is formed. In the sample that coated in 30 min, there are no considerable changes relative to the coating fabricated in 20 min. As it is observed in Fig. 5 d, by further increase in treatment time to 40 min, the crystals of

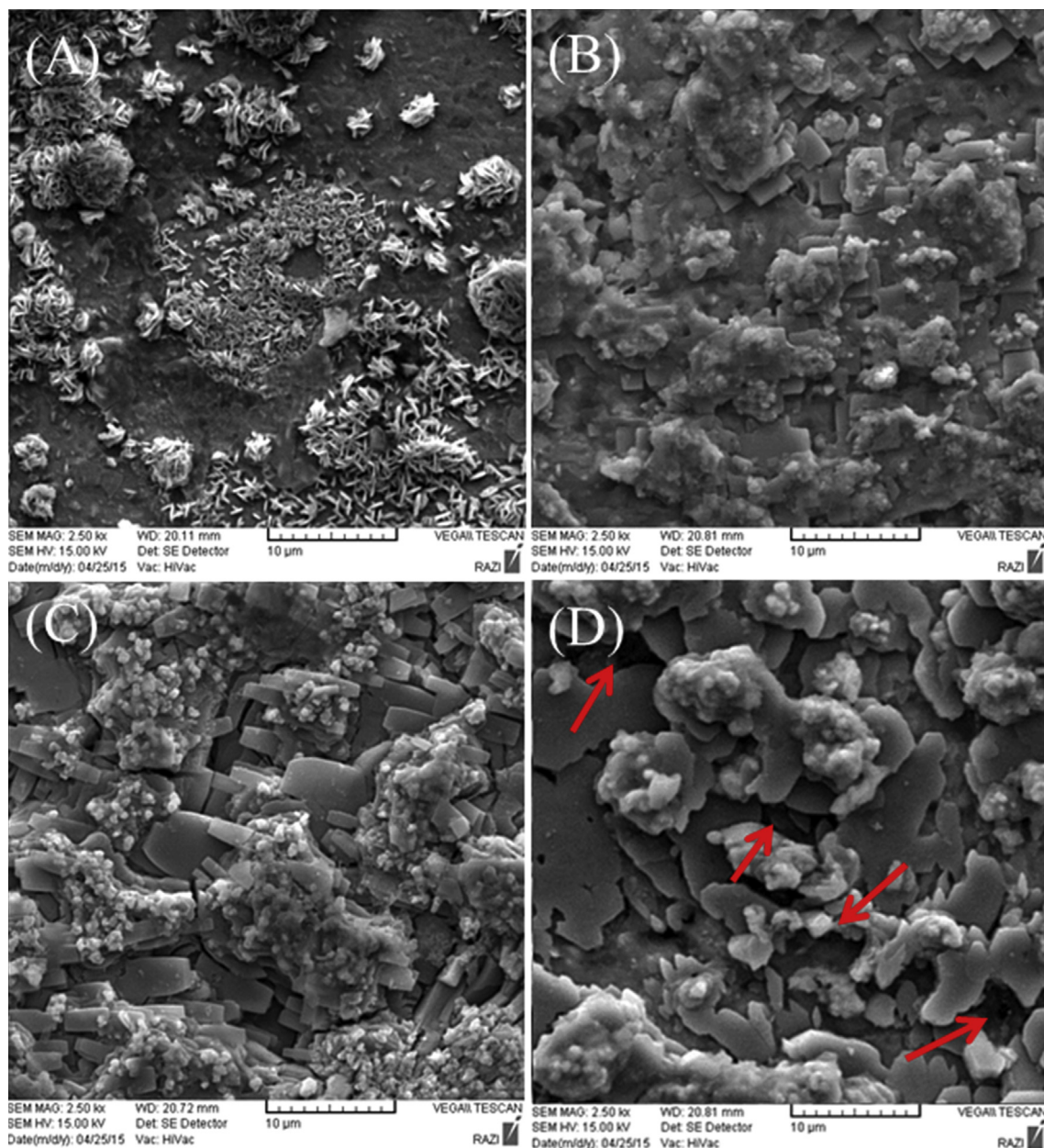


Fig. 3. SEM images of Zn-Ni phosphate coating obtained at different temperatures A) 27 °C, B) 40 °C, C) 50 °C, D) 60 °C.

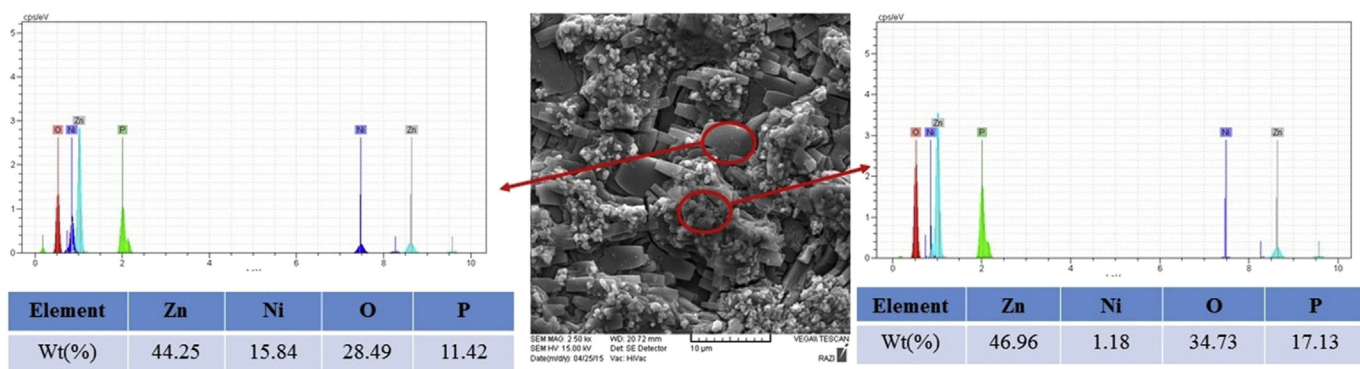


Fig. 4. EDS analysis of the Zn-Ni phosphate coating in the flower-like and plate-like crystals.

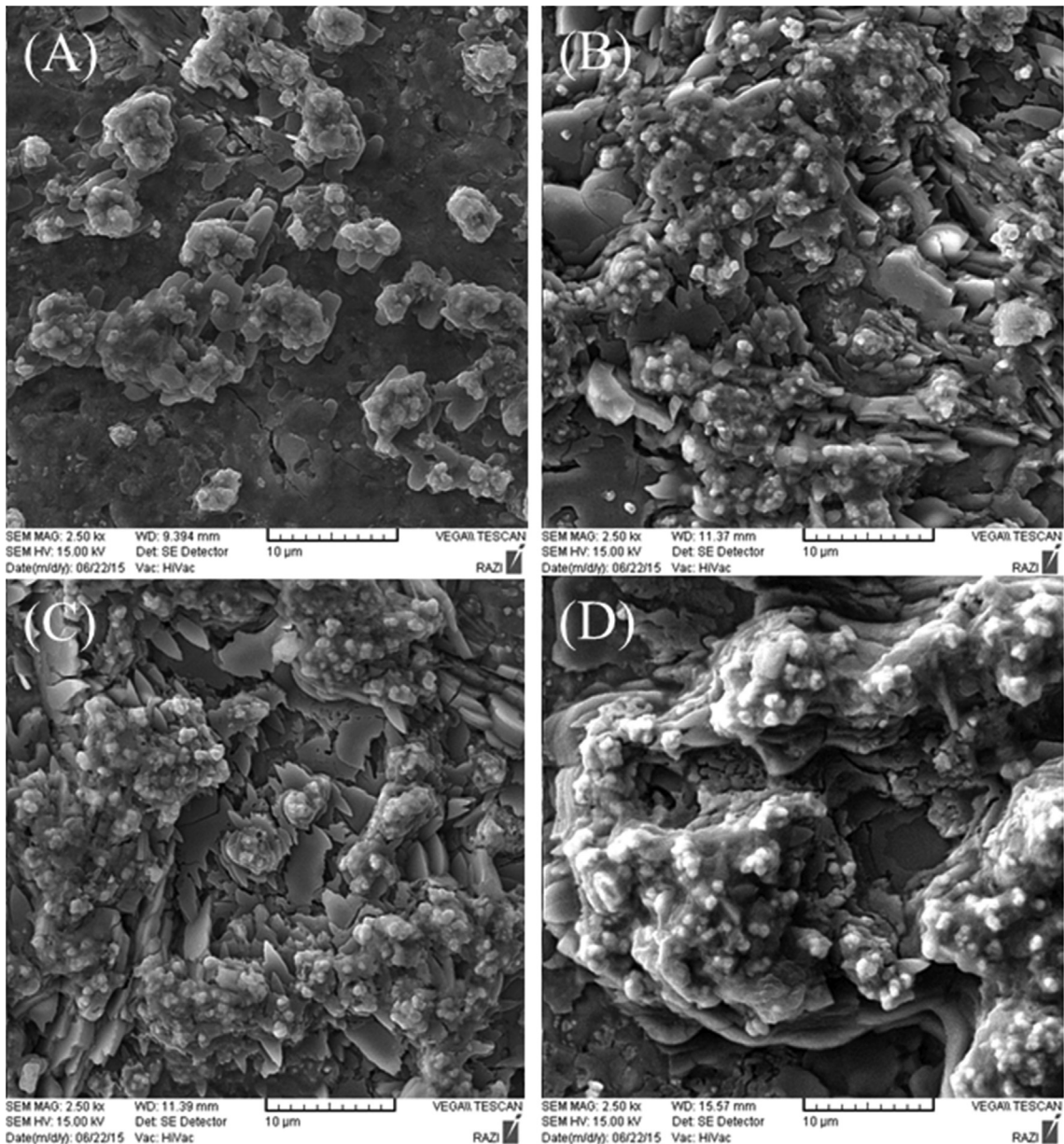


Fig. 5. SEM images of Zn-Ni phosphate coating obtained at different times A) 10 min, B) 20 min, C) 30 min, D) 40 min.

coating have grown and by an increase in phosphate crystal size, distances between crystals have also grown. This cause increase in porosity of coating which is indicated in Fig. 5 d. The variation of coating thickness as a function of electrolyte temperature in various phosphating time is presented in Fig. 6. As it is observed, in constant phosphating time the thickness of the coating increases by increasing the phosphating temperature until 50 °C, thereafter the thickness of coating starts to decrease with increasing the bath temperature. The cause of the increase in thickness in temperature range between 27 and 50 °C is rise in driving force for coating growth due to an increase in electrolyte temperature. The cause of the decrease in phosphate thickness after 50 °C is maybe dissolution of coating at high temperature. As it is observed in constant temperature, by increasing the phosphating time, the thickness of the coating increased due to the formation of more phosphate crystals at high treatment time.

3.3. Corrosion behavior

3.3.1. Immersion in 3.5% NaCl

Immersion in 3.5% NaCl solution is a simple test which provides an appropriate insight into the corrosion behavior of the coating. In this test, the amount of corrosion is assessed by visual observation after 12 h of immersion and by measuring the loss in mass due to the corrosion after 24 h of immersion. Observation after 12 h indicated that the cathodically formed phosphate coating remains in good conditions. One of the observations after immersion test is the formation of white rust on the surface of the coating. The cause of this observation is the presence of elemental zinc in the coating which reacts with an electrolyte that diffused in the pores of the coating. Jegannathan et al. [13] are also observed the formation of white rust corrosion product in the zinc phosphate coating obtained by the cathodic electrochemical method. Deposition of zinc oxide and hydroxide in the cathodically formed phosphate coating

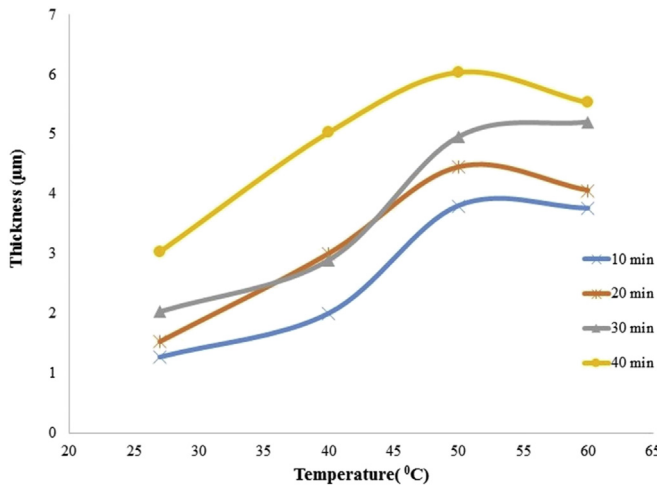


Fig. 6. Variation of coating thickness as a function of phosphating time and temperature.

improve the protective ability of the fabricated coating [13]. The loss in weight of the coating due to the corrosion is measured after 24 h immersion in 3.5% NaCl solution and the results of coating which fabricated at different times and different temperatures are presented in Table 2 and Table 3 respectively. As it is seen, the lowest loss in weight corresponds to best corrosion resistance which is obtained in 50 °C and 30 min electrophosphating treatments.

3.3.2. Potentiodynamic polarization studies

Corrosion behavior of Zn-Ni phosphate coating obtained by the cathodic electrochemical method at different phosphating times and temperatures were characterized using potentiodynamic polarization test. The potentiodynamic polarization curves of the coating obtained at divers times and temperatures are represented in Fig. 7 and Fig. 8, respectively.

The electrochemical parameters such as corrosion potential (E_{corr}), corrosion current density (i_{corr}) and cathodic and anodic slopes are calculated from linear polarization method for coating which obtained at different temperatures are reported in Table 4. As it is seen, by increasing the temperature of the bath from 27 °C to 40 °C, the corrosion current density decrease from 10.71 $\mu\text{A}/\text{cm}^2$ to 1.04 $\mu\text{A}/\text{cm}^2$ and by increasing the temperature from 40 °C to 60 °C the corrosion current density increases to 2.3 $\mu\text{A}/\text{cm}^2$. This indicated the best corrosion resistance of the coating can be obtained in a temperature range between 40 and 50 °C. Two of the main factors affecting the corrosion resistance of the coating are morphology and microstructure of coating [28]. As it was seen, the coating which is fabricated at 27 °C, has a small needle-like phosphate crystals that are not fully cover the entire surface of the substrate and give rise to penetration of aggressive ions into the substrate and, consequently poor corrosion resistance of the coating. The coatings which are formed at 40 and 50 °C have the lowest porosity and the phosphate crystals are fully covered the surface of the substrate. In this situation, penetration of aggressive ions into the substrate is strongly limited and consequently the high corrosion resistance can be obtained. The high porosity of the coating which

Table 3
Loss in weight of coatings fabricated at different temperatures.

Temperature (°C)	27	40	50	60
Loss in weight (g/m^2)	6.23	1.2	0.7	4.7

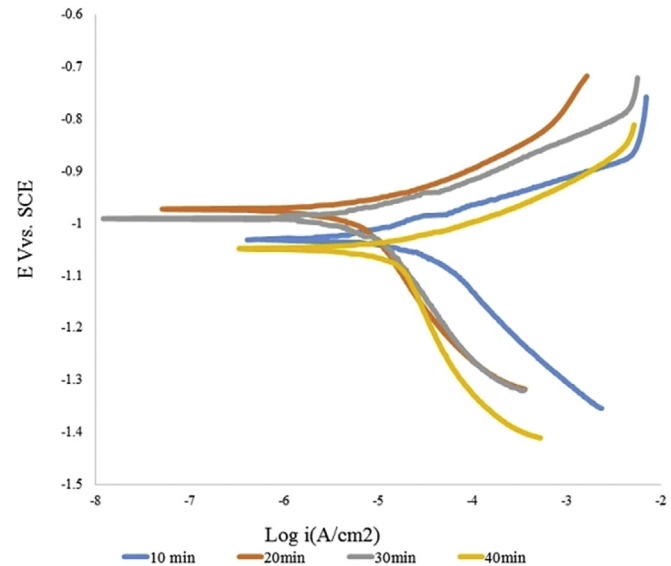


Fig. 7. Potentiodynamic polarization of the Zn-Ni phosphate coating formed at different phosphating times.

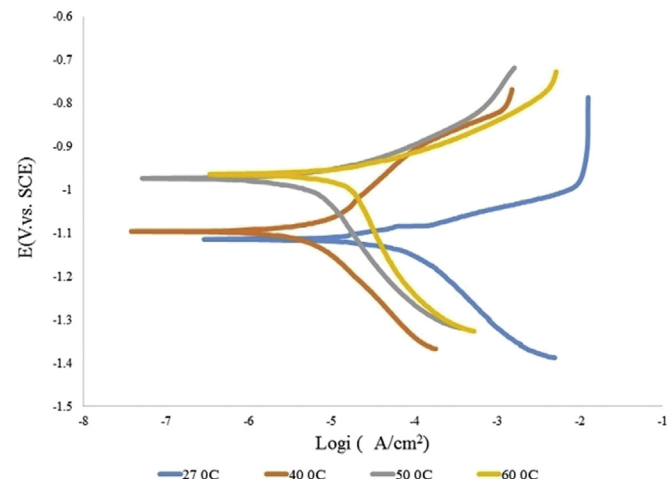


Fig. 8. Potentiodynamic polarization of the Zn-Ni phosphate coating formed at different phosphating temperatures.

is formed at high temperature leading to the poor corrosion resistance of this coating.

The electrochemical parameters for coating which obtained at different times are reported in Table 5. As it is seen in Table 4, by increasing the phosphating time from 10 min to 20 min, the corrosion current density decreases from 4.12 to 0.68 $\mu\text{A}/\text{cm}^2$ and by increasing the phosphating time to 40 min the corrosion current density increases to 5.3 $\mu\text{A}/\text{cm}^2$. This indicated that the range of phosphating time to obtain the coating with the best corrosion resistance is between 20 and 30 min. As it was observed, the coating which was fabricated at 10 min, had high porosity and the phosphate crystals in this situation can not cover the entire surface

Table 2
Loss in weight of coatings fabricated at different time.

Time (min)	10	20	30	40
Loss in weight (g/m^2)	7.43	1.7	1.3	5.3

Table 4

Results of polarization tests of coatings fabricated at various temperature.

Temperature (°C)	i_{corr} ($\mu\text{A}/\text{cm}^2$)	E_{corr} (mV vs.SCE)	β_a (mV/decade)	β_c (mV/decade)	R_p ($\Omega \cdot \text{cm}^2$)
27°	10.71	−1096	17.6	16.5	354.7
40	1.04	−1095	17	19	3740
50	0.73	−972	13	16	3533
60	2.3	−963	12	11	1324

Table 5

Results of polarization tests of coating which fabricated at different time.

Time (min)	i_{corr} ($\mu\text{A}/\text{cm}^2$)	E_{corr} (mV vs.SCE)	β_a (mV/decade)	β_c (mV/decade)	R_p ($\Omega \text{ cm}^2$)
10	4.12	−1044	17	21	1254
20	0.68	−991	14	13	3481
30	1.87	−990	27	34	3156
40	2.54	−1048	12	15	1324

of substrate, then the coating with low corrosion resistance was formed at 10 min phosphating time. The coating that is formed at the 20 and 30 min have the compact phosphate crystals and the porosities of these coating are very low leading to a coating with the best corrosion resistance, and finally high porosity of the coating that is formed at 40 min results in a coating with poor corrosion resistance. It is worth noting that, as can be seen, the results of immersion test are completely consistent with the results of polarization studies.

3.3.3. Electrochemical impedance spectroscopy studies

Electrochemical impedance spectroscopy test was also performed to obtain more information about corrosion resistance and corrosion mechanism of the Zn-Ni electrophosphate coating obtained by cathodic electrochemical method. Nyquist plot of the coating which is fabricated at different temperature and times are represented in Fig. 9 and Fig. 10, respectively. An equivalent circuit proposed for the coatings which are formed at 27, 40 and 50 °C and the coating which are formed at 10, 20 and 30 min, is shown in Fig. 11 in which R_s is solution resistance, R_p is charge transfer resistance, CPE_{dl} is the double layer capacitance and W is the Warburg diffusion element in the equivalent circuit. Here a more general term of constant phase element is used instead of the capacitor. The use of constant phase element (CPE) in the equivalent circuit of the impedance not only minimizes the systematical error, but also provides more detailed information about the non-ideal di-electrical properties of the coating. The impedance function of CPE element is defined by Eq (8).

$$Z = \frac{(j\omega)^{-n}}{Y_0} \quad (8)$$

In which Y_0 and n are the admittance and empirical exponent of the CPE, respectively, j is an imaginary number and ω is the angle frequency. For n = 1, an ideal capacitor is defined. For n = 0, the CPE represents an ideal resistor. For n = −1, the CPE is equivalent with an inductance [29,30]. As it is seen in Figs. 9 and 10, the Nyquist plot of the coated samples in the coating which are formed at 27, 40 and 50 °C and 10, 20 and 30 min, exhibit a semicircle in the high-frequency region followed by a typical Warburg impedance behavior at the low-frequency region, suggesting that the corrosion of coated samples in this conditions is under diffusion control. The diffusion control of corrosion of coating can be related to nature of the coating. As stated earlier, the Zn-Ni phosphate coating which is fabricated using the cathodic electrochemical method can be classified as Zn-Ni phosphate composite coating in which the elemental zinc is presented along with phosphate crystals. The presence of elemental zinc in the coating leads to the formation of zinc base corrosion products. This corrosion product also observed in the immersion test. Jegannathan et al. [13] suggested that the zinc corrosion products may consist of zinc oxide and zinc hydroxy chloride. It has also been reported that the mixed salt

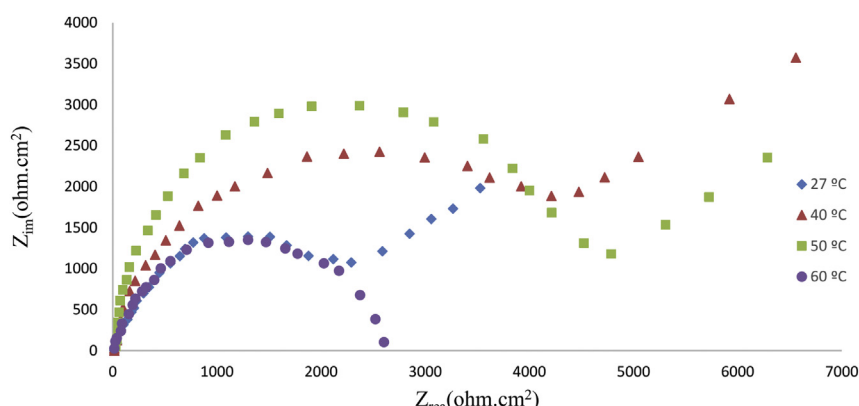


Fig. 9. Nyquist plots of the Zn-Ni phosphate coating formed at different phosphating temperatures.

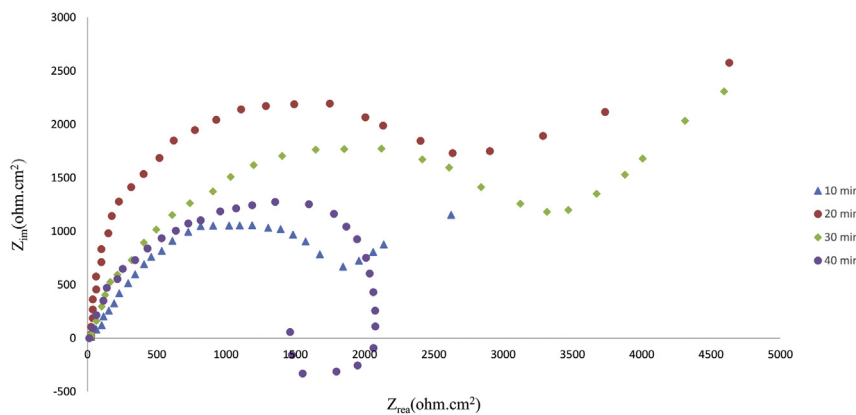


Fig. 10. Nyquist plots of the Zn-Ni phosphate coating formed at different phosphating times.

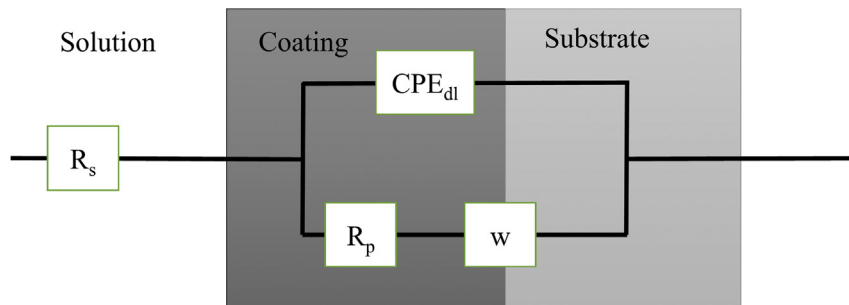


Fig. 11. Equivalent circuit proposed for the coating which is formed at 27, 40 and 50 °C and the coating which are formed at 10, 20 and 30 min.

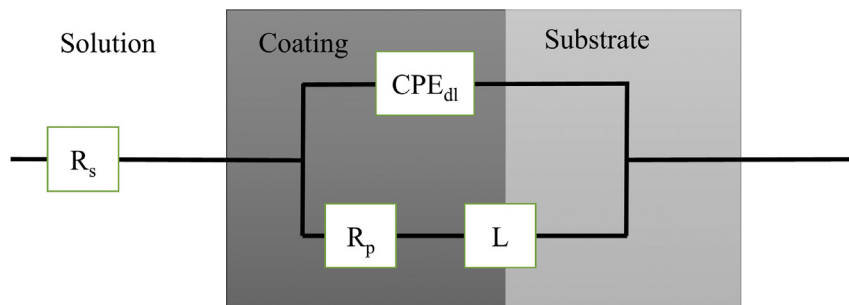


Fig. 12. Equivalent circuit proposed for the coating which is formed at 40 min.

$4\text{Zn}(\text{OH})_2 \cdot \text{ZnCl}_2$ is formed in samples exposed to industrial atmospheres. Corrosion products are formed in the coating which prevents the penetration of aggressive ions into the substrate and diffusion of aggressive ions in the corrosion products control the overall reaction rate. Thus in this condition, the corrosion of coated sample is under diffusion control. Therefore, it can be concluded

that the presence of phosphate crystals and elemental zinc in the composition of phosphate layer obtained by cathodic electrochemical method provides both sacrificial and barrier protection for substrate and thereby improves the corrosion resistance of the coating. In the coating that is formed at 60 °C, the control diffusion behavior is not observed due to the high porosity of the coating. In

Table 6

Results of EIS test of the coating which are formed at different conditions.

Type of studied system	R_s (ohm cm ²)	R_p (ohm cm ²)	CPE_{dl} (ohm ⁻¹ cm ⁻² s ⁿ)
Cathodically phosphated galvanized steel at 27 °C	15.26	13123	3.6×10^{-8}
Cathodically phosphated galvanized steel at 40 °C	18.24	32156	6.4×10^{-8}
Cathodically phosphated galvanized steel at 50 °C	27.36	45236	8.3×10^{-8}
Cathodically phosphated galvanized steel at 60 °C	15.3	36125	4.2×10^{-8}
Cathodically phosphated galvanized steel at 10 min	12.69	19362	2.4×10^{-8}
Cathodically phosphated galvanized steel at 20 min	32.45	42164	4.8×10^{-8}
Cathodically phosphated galvanized steel at 30 min	16.32	47526	7.2×10^{-8}
Cathodically phosphated galvanized steel at 40 min	12.36	17236	3.6×10^{-8}

the coating which is formed at 40 min, the inductive loop is observed at the low-frequency region. The equivalent circuit of this coating is represented in Fig. 12. The cause of this inductive loop can be related to the dissolution of coating or very high porosity of the coating in this condition. Table 6 represent the EIS simulation results of the various electrophosphate galvanized steel at different conditions. As it is seen in this table, by increasing the phosphating time from 10 to 20, R_p increased suggesting the increase in the corrosion resistance and by further increasing in phosphating time, R_p decreased suggesting the decrease in corrosion resistance of the coating that is formed at high phosphating time. And results of EIS studies indicated that the highest R_p is obtained in the temperatures range between 40 and 50 °C which is in good agreement with the polarization and immersion tests results.

4. Conclusion

Zn-Ni electrophosphate coating was applied on galvanized steel using the cathodic electrochemical method and the effect of phosphating times and temperatures on corrosion behavior and microstructure of coating were investigated. The main results of this study can be summarized as follow:

- 1 Zn-Ni phosphate coating which is obtained by cathodic electrochemical method can be classified as Zn-Ni phosphate composite coating due to the presence of elemental zinc and nickel along with zinc phosphate and nickel phosphate.
- 2 The best corrosion resistance of the coating is obtained in the range of temperatures between 40 and 50 °C as a result of compact phosphate coating.
- 3 The best corrosion resistance of the coating is obtained in the range of times between 20 and 30 min due to compact phosphate coating.
- 4 Results of EIS studies indicated that the corrosion of coated samples are under diffusion control due to the formation of zinc base corrosion products.
- 5 Presence of phosphate crystals and elemental zinc in the composition of phosphate layer obtained by cathodic electrochemical method provides both sacrificial and barrier protection for substrate and thereby improves the corrosion resistance of the coating.

References

- [1] H.-Y. Su, C.-S. Lin, Effect of additives on the properties of phosphate conversion coating on electrogalvanized steel sheet, *Corros. Sci.* 83 (2014) 137–146.
- [2] C.-Y. Tsai, J.-S. Liu, P.-L. Chen, C.-S. Lin, A two-step roll coating phosphate/molybdate passivation treatment for hot-dip galvanized steel sheet, *Corros. Sci.* 52 (2010) 3385–3393.
- [3] C.-Y. Tsai, J.-S. Liu, P.-L. Chen, C.-S. Lin, Effect of Mg 2+ on the microstructure and corrosion resistance of the phosphate conversion coating on hot-dip galvanized sheet steel, *Corros. Sci.* 52 (2010) 3907–3916.
- [4] B.-L. Lin, J.-T. Lu, G. Kong, Effect of molybdate post-sealing on the corrosion resistance of zinc phosphate coatings on hot-dip galvanized steel, *Corros. Sci.* 50 (2008) 962–967.
- [5] M. Wolpers, J. Angeli, Activation of galvanized steel surfaces before zinc phosphating—XPS and GDOES investigations, *ApSS* 179 (2001) 281–291.
- [6] Y.-y. Xu, B.-l. Lin, Effect of silicate pretreatment, post-sealing and additives on corrosion resistance of phosphated galvanized steel, *Trans. Nonferrous Metals Soc. China* 17 (2007) 1248–1253.
- [7] T.S. Narayanan, Surface pretreatment by phosphate conversion coatings—a review, *Rev. Adv. mater. Sci.* 9 (2005) 130–177.
- [8] E. Banczek, P. Rodrigues, I. Costa, The effects of niobium and nickel on the corrosion resistance of the zinc phosphate layers, *SuCT* 202 (2008).
- [9] T.-T. Chen, S.-T. Ke, Y.-M. Liu, K.-H. Hou, The study on optimizing the zinc phosphate conversion coating process and its corrosion resistance, *J. Chung Cheng Inst. Technol.* 34 (2006) 1–11.
- [10] G. Li, L. Niu, J. Lian, Z. Jiang, A black phosphate coating for C1008 steel, *SuCT* 176 (2004) 215–221.
- [11] S. Jegannathan, T. Arumugam, T.S. Narayanan, K. Ravichandran, Formation and characteristics of zinc phosphate coatings obtained by electrochemical treatment: cathodic vs. anodic, *PORCo* 65 (2009) 229–236.
- [12] S. Jegannathan, T.S. Narayanan, K. Ravichandran, S. Rajeswari, Formation of zinc phosphate coating by anodic electrochemical treatment, *SuCT* 200 (2006) 6014–6021.
- [13] S. Jegannathan, T.S. Narayanan, K. Ravichandran, S. Rajeswari, Performance of zinc phosphate coatings obtained by cathodic electrochemical treatment in accelerated corrosion tests, *Electrochim. Acta* 51 (2005) 247–256.
- [14] T.S. Narayanan, S. Jegannathan, K. Ravichandran, Corrosion resistance of phosphate coatings obtained by cathodic electrochemical treatment: role of anode—graphite versus steel, *PORCo* 55 (2006) 355–362.
- [15] C. Kavitha, T.S. Narayanan, K. Ravichandran, I.S. Park, M.H. Lee, Deposition of zinc-zinc phosphate composite coatings on steel by cathodic electrochemical treatment, *J. Coatings Technol. Res.* 11 (2014) 431–442.
- [16] D. Zimmermann, A. Munoz, J. Schultze, Formation of Zn–Ni alloys in the phosphating of Zn layers, *SuCT* 197 (2005) 260–269.
- [17] A. Akhtar, D. Susac, P. Glaze, K. Wong, P. Wong, K. Mitchell, The effect of Ni 2+ on zinc phosphating of 2024-T3 Al alloy, *SuCT* 187 (2004) 208–215.
- [18] A. Akhtar, K. Wong, K. Mitchell, The effect of pH and role of Ni 2+ in zinc phosphating of 2024-Al alloy: Part I: macroscopic Studies with XPS and SEM, *ApSS* 253 (2006) 493–501.
- [19] C.-M. Wang, H.-C. Liau, W.-T. Tsai, Effects of temperature and applied potential on the microstructure and electrochemical behavior of manganese phosphate coating, *SuCT* 201 (2006) 2994–3001.
- [20] M. Fouladi, A. Amadeh, Effect of phosphating time and temperature on microstructure and corrosion behavior of magnesium phosphate coating, *Electrochim. Acta* 106 (2013) 1–12.
- [21] N. Van Phuong, S. Moon, D. Chang, K.H. Lee, Effect of microstructure on the zinc phosphate conversion coatings on magnesium alloy AZ91, *ApSS* 264 (2013) 70–78.
- [22] G. Li, J. Lian, L. Niu, Z. Jiang, Influence of pH of phosphating bath on the zinc phosphate coating on AZ91D magnesium alloy, *Adv. Eng. Mater.* 8 (2006) 123–127.
- [23] A. Oskuiie, A. Afshar, H. Hasannejad, Effect of current density on DC electrochemical phosphating of stainless steel 316, *SuCT* 205 (2010) 2302–2306.
- [24] S. Shamugam, K. Ravichandran, T.S. Narayanan, M.H. Lee, A facile electrochemical approach for the deposition of iron–manganese phosphate composite coatings on aluminium, *RSC Adv.* 5 (2015) 988–1008.
- [25] G.B. Darband, A. Afshar, A. Aliabadi, Zn–Ni Electrophosphating on galvanized steel using cathodic and anodic electrochemical methods, *SuCT* (2016) [in press].
- [26] C. Kavitha, T.S. Narayanan, K. Ravichandran, M.H. Lee, Deposition of zinc–zinc phosphate composite coatings on aluminium by cathodic electrochemical treatment, *SuCT* 258 (2014) 539–548.
- [27] J. Flis, Y. Tobiyama, C. Shiga, K. Mochizuki, Behaviour of intact and scratched phosphate coatings on zinc, zinc–nickel and mild steel in dilute sodium phosphate solution, *JApEl* 32 (2002) 401–407.
- [28] M. Aliokhzraei, R.S. Gharabagh, M. Teimouri, M. Ahmadzadeh, G.B. Darband, H. Hasannejad, Ceria embedded nanocomposite coating fabricated by plasma electrolytic oxidation on titanium, *JAlIC* 685 (2016) 376–383.
- [29] F. Mansfeld, Recording and analysis of AC impedance data for corrosion studies, *Corrosion* 37 (1981) 301–307.
- [30] E. Van Westing, G. Ferrari, J. De Wit, The determination of coating performance with impedance measurements—I. Coating polymer properties, *Corros. Sci.* 34 (1993) 1511–1530.
- [31] Y. Hao, F. Liu, E.-H. Han, S. Anjum, G. Xu, The mechanism of inhibition by zinc phosphate in an epoxy coating, *Corros. Sci.* 69 (2013) 77–86.